Vol. 128: 37–49, 2018
https://doi.org/10.3354/dao03210

DISEASES OF AQUATIC ORGANISMS
Dis Aquat Org

Published March 22

# New myxosporeans parasitizing *Phractocephalus hemioliopterus* from Brazil: morphology, ultrastructure and SSU-rDNA sequencing

**Juliana Naldoni[1,*], Antônio A. M. Maia[2], Lincoln L. Correa[3], Marcia R. M. da Silva[2], Edson A. Adriano[1,4]**

[1]Departamento de Ecologia e Biologia Evolutiva, Universidade Federal de São Paulo (UNIFESP), Rua Professor Artur Riedel, 275, Jardim Eldorado, CEP 09972-270, Diadema, SP, Brazil

[2]Departamento de Medicina Veterinária, Faculdade de Zootecnia e Engenharia de Alimentos, Universidade de São Paulo (USP), Rua Duque de Caxias Norte, 225, CEP 13635-900, Pirassununga, SP, Brazil

[3]Instituto de Ciências e Tecnologia das Águas, Universidade Federal do Oeste do Pará (UFOPA), Travessa Professor Antônio Carvalho Fátima, CEP 68040470, Santarém, PA, Brazil

[4]Departamento de Biologia Animal, Universidade Estadual de Campinas (UNICAMP), Rua Monteiro Lobato, 255, CEP 13083-970, Campinas, SP, Brazil

ABSTRACT: Myxozoans are a diverse group of parasitic cnidarians, with some species recognized as serious pathogens to their hosts. The present study describes 2 new myxobolid species (*Myxobolus figueirae* sp. nov. and *Henneguya santarenensis* sp. nov.) infecting skin and gill filaments of the Amazonian pimelodid fish *Phractocephalus hemioliopterus*, based on ultrastructural, histology and phylogenetic analysis. The fish were caught in the Amazon River, Pará, Brazil. The plasmodial development of *M. figueirae* sp. nov. was in the dermis and those of *H. santarenensis* sp. nov. were of the intralamellar type. For both species, the plasmodia were surrounded by a connective tissue layer, but there was no inflammatory infiltrate. For *M. figueirae* sp. nov., mature spores were ovoid measuring 9.1 to 10 (9.5 ± 0.3) µm in length, 5.8 to 6.9 (6.4 ± 0.3) µm in width and 4.4 to 4.5 (4.5 ± 0.1) µm in thickness. Two polar capsules were elongated and of unequal size. For *H. santarenensis* sp. nov., mature spores were ellipsoidal in the frontal view, measuring 26.3 to 36.1 (31.9 ± 3) µm in total length, 9.6 to 11.9 (10.8 ± 0.5) µm in body length, 3.7 to 4.9 (4.3 ± 0.3) µm in width and 16.6 to 25.6 (21 ± 3.1) µm in caudal process. The polar capsules were elongated and of equal size. Phylogenetic analysis, based on partial small subunit ribosomal DNA (SSU rDNA) sequences and using the closest myxozoan sequences to each one of the species studied here based on previous GenBank data, showed *M. figueirae* sp. nov. and *H. santarenensis* sp. nov. clustering in distinct lineages. While *H. santarenensis* sp. nov. clustered in a well-supported subclade composed of *Henneguya* species that infect gills of South American pimelodid hosts, *M. figueirae* sp. nov. clustered in a weakly supported subclade containing parasite species of bryconid hosts.

KEY WORDS: Myxosporea · *Myxobolus figueirae* · *Henneguya santarenensis* · Ultrastructure · Histology · Amazon · Brazil



## INTRODUCTION

Myxozoans are reduced cnidarian parasites possessing great diversity, and some species are considered serious potential pathogens for their fish hosts (Feist & Longshaw 2006, Okamura et al. 2015). Presently, about 2400 species are recognized (Zhang 2011). The genera *Myxobolus* Bütschli, 1882 and *Henneguya* Thelohan, 1892 are among the most diverse of that class, respectively harboring around 905

*Corresponding author: jnaldoni@gmail.com

*Myxobolus* species and 192 *Henneguya* (Eiras & Adriano 2012, Eiras et al. 2014). Thus far, 12 myxosporean species have been described in Siluriformes fish from South America, 7 from the *Pseudoplatystoma*, 2 from *Pimelodus* and 1 from *Zungaro* and *Hypophthalmus* genera (Rocha et al. 2014, Naldoni et al. 2014, Carriero et al. 2013, Matos et al. 2005).

The Amazon basin drains about 6.5 million $km^2$ (Goulding 1996) and is a complex ecosystem consisting of highly diverse environments with many biotopes at the disposal of aquatic communities (Santos 1986/1987), providing a favorable habitat for exceptional fish biodiversity — approximately 5000 fish species (Val & Honczaryk 1995). In this context, the family Pimelodidae stands out due to its large diversity and importance to the fishing economy of the region (Lundberg & Littmann 2003, Lundberg et al. 2011, MPA 2012).

The present study describes, based on morphology, ultrastructure and small subunit ribosomal DNA (SSU-rDNA) sequencing, 2 new myxosporean species infecting the skin and gills of *Phractocephalus hemioliopterus*, a large Amazon pimelodid fish of commercial importance to the fishing and aquarium sectors.

## MATERIALS AND METHODS

A total of 7 wild specimens of *Phractocephalus hemioliopterus* were caught in October 2014 in the Tapajos River, in the municipality of Santarém, Pará State, Brazil (2° 26′ 36″ S, 55° 09′ 28″ W), with the aim of analyzing parasites. Fish catches were authorized by the Brazilian Ministry of the Environment (SISBIO No. 44268-4). The fish were transported live to a field laboratory where they were euthanized by benzocaine overdose. The methodology of the present study was approved by the ethics research committee of Federal University of São Paulo (CEUA N 92090802140) in accordance with Brazilian law (Federal Law No. 11794, dated 8 October 2008).

Morphological characterization of the myxobolid species was based on mature spores obtained from 3 different fish specimens. Measurements were performed on 30 spores using an Axioplan 2 Zeiss Microscope and Axivision version 4.1 image capture software. The dimensions of the spores are expressed as mean ± standard deviation (SD), in µm. Smears containing free spores were air-dried and stained with Giemsa solution, and mounted in a low-viscosity mounting medium (Cytoseal™) on permanent slides for archival deposition.

For histological analysis, fragments of infected organs were fixed in 10% buffered formalin and embedded in paraffin. Serial sections with a thickness of 4 µm were stained with hematoxylin-eosin.

For transmission electron microscopy, plasmodia were fixed in 2.5% glutaraldehyde in 0.1 M sodium cacodylate buffer (pH 7.4) for 12 h, washed in a glucose–saline solution for 2 h and post-fixed in $OsO_4$. All these processes were performed at 4°C. After dehydration using an acetone series, the material was embedded in EMbed 812 resin. Semi-thin sections were stained with toluidine blue solution and examined by light microscopy; ultra-thin sections, double-stained with uranyl acetate and lead citrate, were examined in an LEO 906 electron microscope at 60 kV.

For molecular analysis, plasmodia were removed from the host tissue and fixed in absolute ethanol. DNA was extracted from a single plasmodium for both species using the DNeasy® Blood & Tissue kit (Qiagen), following manufacturer's instructions and quantified in a NanoDrop 2000 spectrophotometer (Thermo Scientific). The methodology did not allow detection of intraspecific sequence variation.

Polymerase chain reaction (PCR) was carried out using a final volume of 25 µl, which contained 10 to 50 ng of extracted DNA, 0.2 pmol of each primer, 12.5 µl of DreamTaq Green PCR Master Mix and nuclease-free water (Thermo Fisher Scientific) in an Eppendorf AG 22331 Hamburg Thermocycler (Eppendorf). The SSU-rDNA sequence was amplified with the primer pairs ERIB1 (Barta et al. 1997) — ACT1r (Hallett & Diamant 2001) and TEDf (Capodifoglio et al. 2016) — ERIB10 (Barta et al. 1997), which amplified 2 fragments of approximately 1000 and 1200 bp, respectively. An initial denaturation stage at 95°C for 5 min was followed by 35 cycles of denaturation at 95°C for 60 s, annealing at 58°C for 60 s, extension at 72°C for 90 s, finishing with an extended elongation stage at 72°C for 5 min. PCR products were electrophoresed in 1.0% agarose gel, stained with Sybr Safe DNA gel stain (Invitrogen by Life Technologies) and analyzed by an LED transilluminator (Kasvi).

PCR products were purified with QIAquick® PCR Purification Kit (Qiagen). The sequencing was performed with the same primer pairs used in the amplification stage, plus primers MC5 and MC3 (Molnár et al. 2002) and using the BigDye® Terminator v3.1 Cycle Sequencing Kit (Applied Biosystems) in an ABI 3730 DNA sequencing analyzer (Applied Biosystems). The sequence obtained was visualized, assembled and edited using BioEdit 7.1.3.0 software (Hall 1999). A standard nucleotide BLAST (blastn) search

was conducted to verify the similarity of the sequence obtained in this study with other sequences available in the GenBank database (Altschul et al. 1997). Phylogenetic analysis was performed using the closest myxozoan sequences to each one of the species studied here based on previous GenBank data. This included 25 sequences of *Henneguya* species, 31 sequences of *Myxobolus*, 9 sequences of *Thelohanellus* species and 2 of *Unicauda* species. *Ceratomyxa vermiformes* and *C. amazonensis* were used as the outgroup. Nucleotide sequences were aligned using ClustalW within BioEdit version 7.0.9.0 (Hall 1999). Phylogenetic analysis was conducted using maximum likelihood (ML) in PhyML software (Guindon et al. 2010), with NNI search, automatic model selection by SMS (Smart Model Selection), under a GTR + G + I substitution model (with 6 categories), equilibrium frequencies optimized, transition/transversion ratio estimated, proportion of invariable sites fixed (0.240) and Gamma shape parameter fixed (0.580). Bootstrap analysis (1000 replicates) was employed to assess the relative robustness of the tree branches. The resulting tree was visualized with FigTree v1.3.1 (Rambaut 2008). Only bootstrap values above 50 were considered to be well supported. The data for the family of host fish was obtained from Froese & Pauly (2013). Other alignments, including aligning the most closely related myxosporean species to each one of the new species in the phylogenetic tree, was completed to produce pairwise similarity matrices using MEGA 6.0 (Tamura et al. 2013).

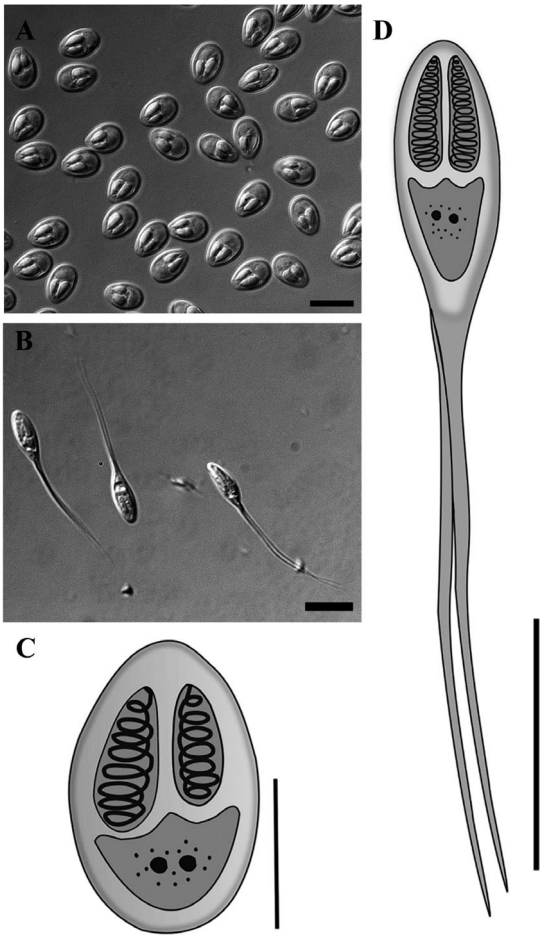


Fig. 1. Myxosporeans infecting *Phractocephalus hemioliopterus*. (A,B) Mature spores (frontal view) under differential interference contrast optics and (C,D) schematic representations. (A) *Myxobolus figueirae* sp. nov. found in the skin. Scale bar = 10 µm; (B) *Henneguya santarenensis* sp. nov. infecting the gill. Scale bar = 10 µm; (C) *M. figueirae* sp. nov. Scale bar = 5 µm; (D) *H. santarenensis* sp. nov. Scale bar = 10 µm

## RESULTS

From 7 specimens of *Phractocephalus hemioliopterus* examined, 3 (43%) had plasmodia harboring spores corresponding to *Myxobolus* genus in the skin, and all 7 (100%) had plasmodia harboring spores corresponding to *Henneguya* genus in the gill (Fig. 1). The present study was performed on wild fish, and no pathogenic effects of these myxosporeans was observed on the studied specimens. The analysis and our literature review showed that both were novel species; their descriptions are provided below.

### *Myxobolus figueirae* sp. nov.

**Morphology:** Plasmodia, white and spherical measuring up to 3 mm in diameter. Mature spores ovoid in frontal view, measuring 9.1 to 10 (9.5 ± 0.3) µm in length, 5.8 to 6.9 (6.4 ± 0.3) µm in width and 4.4 to 4.5 (4.5 ± 0.1) µm in thickness (Fig. 1A, Table 1). In lateral view, spores biconvex, with symmetrical valves. Two elongated polar capsules of different size, the larger measuring 3.5 to 4.6 (4.1 ± 0.3) µm in length and 1.7 to 2.6 (2.1 ± 0.3) µm in width and the smaller, 2.4 to 3.6 (3.2 ± 0.3) µm in length and 1.2 to 2.1 (1.4 ± 0.2) µm in width. Polar tubules have 7 to 8 coils arranged perpendicularly to the longitudinal axis of polar capsule (Figs. 1A,C & 2B).

Histological analysis revealed that the plasmodia develops in the dermis, surrounded by a layer of connective tissue, and this in turn leads to a stretching of the epithelium (Fig. 3). Ultrastructural analysis

Table 1. Comparative data of *Myxobolus figueirae* sp. nov. and *Henneguya santarenensis* sp. nov. with the most morphologically similar *Myxobolus/Henneguya* spp. parasites of fish worldwide and all *Myxobolus/Henneguya* spp. parasites of pimelodids from South America. Spore dimensions, infection sites and collection sites are given. NCT: number of coils of polar tubules; (–) no data. All measurements are means ± SD (in µm) or range

| Species | Total length | Spore | | | Polar capsule | | Tail length | NCT | Site of infection and host | Locality |
|---|---|---|---|---|---|---|---|---|---|---|
| | | Length | Width | Thickness | Length | Width | | | | |
| ***Myxobolus* spp.** | | | | | | | | | | |
| *M. figueirae* sp. nov. | | 9.5 ± 0.3 | 6.4 ± 0.3 | 4.5 ± 0.1 | 4.1 ± 0.3 | 2.1 ± 0.3 | | 8 | Skin of *Phractocephalus hemioliopterus* | Amazon Basin, Brazil |
| | | | | | 3.2 ± 0.3 | 1.4 ± 0.2 | | 7 | | |
| *M. sangei* | | 10.1 | 6.2 | 1.6 | 6.2 | 2.2 | | 7–8 | Gills, skin and kidney of *Brycinus macrolepidotus* | Cameroon, Africa |
| | | | | | 4.8 | 1.7 | | 4–5 | | |
| *M. axelrodi* | | 20.5 ± 0.7 | 6.6 ± 0.5 | 5.1 ± 0.4 | 9.9 ± 0.8 | 3.8 ± 0.3 | | – | Brain of *Paracheirodon axelrodi* | Brazil |
| | | | | | 3.8 ± 0.3 | 2.0 ± 0.1 | | – | | |
| *M. flavus* | | 9.2 ± 0.2 | 6.5 ± 0.3 | 4.2 ± 0.2 | 4.5 ± 0.2 | 1.6 ± 0.1 | | 4–5 | Gill arch of *Pseudoplatystoma corruscans* | Pantanal wetland, Brazil |
| *M. flavus* | | 9.3 ± 0.3 | 6.6 ± 0.3 | 4.0 ± 0.2 | 4.5 ± 0.2 | 1.8 ± 0.1 | | 4–5 | Gill arch of *Pseudoplatystoma reticulatum* | Pantanal wetland, Brazil |
| *M. absonus* | | 15.7 ± 1.5 | 10.2 ± 0.7 | – | 6.4 ± 0.7 | 3.6 ± 0.5 | | 5 | Opercular cavity of *Pimelodus maculatus* | Piracicaba River, Brazil |
| *M. cordeiroi* | | 10.8 ± 0.5 | 7.1 ± 0.2 | 5.2 ± 0.3 | 5.2 ± 0.3 | 1.4 ± 0.1 | | 5–6 | Skin, gill arch, eyes, urinary bladder of *Zungaro jahu* | Pantanal, Brazil |
| *M. stokesi* | | 8.5 | 5.3 | – | 3.1 | 1.7 | | | Nose integument of *Pimelodella* (?) sp. | Brazil |
| *M. sciades* | | 9.15 | 4.36 | 2.61 | 4.44 | 1.63 | | 9–10 | Gill of *Sciades herzbergii* | Brazil |
| *M. umidus* | | 13.5 ± 0.7 | 7.8 ± 0.4 | 7.7 ± 0.1 | 5.1 ± 0.4 | 2.7 ± 0.3 | | 4–5 | Spleen of *Brycon hilarii* | Pantanal wetland, Brazil |
| *M. macro-plasmodialis* | | 11 | 8.5 | 5.2 | 4.5 | 2.8 | | 6 | Abdominal cavity of *Salminus maxillosus* (= *S. brasiliensis*) | Mogi Guaçu River, Brazil |
| *M. batalhensis* | | 15.2 ± 0.8 | 8.5 ± 0.5 | 5.2 ± 0.3 | 5.2 ± 0.3 | 2.8 ± 0.2 | | 6–9 | Ovary of *Salminus hilarii* | Brazil |
| *M. batalhensis* | | 15.3 ± 0.9 | 8.3 ± 0.3 | 5.0 ± 0.1 | 5.4 ± 0.1 | 2.8 ± 0.1 | | 6–9 | Liver of *Salminus hilarii* | Brazil |
| *M. cf. colossomatis* | | 10.3 ± 0.7 | 6.4 ± 0.8 | – | 4.4 ± 0.42 | 1.8 ± 0.22 | | 7–8 | Gills of *Piaractus mesopotamicus* | Fish farm in São Paulo, Brazil |
| ***Henneguya* spp.** | | | | | | | | | | |
| *H. santarenensis* sp. nov. | 31.9 ± 3 | 10.8 ± 0.5 | 4.3 ± 0.3 | 3.6 ± 0.2 | 4.6 ± 0.4 | 1.4 ± 0.2 | 21 ± 3.1 | 15 | Lamella of *Phractocephalus hemioliopterus* | Amazon Basin, Brazil |
| *H. cuniculator* | 29.4 ± 1.9 | 12.13 ± 0.69 | 4.8 ± 0.29 | 4.23 ± 0.15 | 6.18 ± 0.28 | 1.8 ± 0.12 | 16.7 ± 1.9 | 10–11 | Gill filaments of *Pseudoplatystoma corruscans* | São Francisco River, Brazil |
| *H. multi-plasmodialis* | 30.8 ± 1.3 | 14.7 ± 0.5 | 5.2 ± 0.3 | 4.4 ± 0.1 | 6.1 ± 0.1 | 1.4 ± 0.1 | 15.4 ± 1.3 | 6–7 | Large cysts in the gills of *Pseudoplatystoma corruscans* | Pantanal wetland, Brazil |
| *H. multi-plasmodialis* | 30.6 ± 1.2 | 14.5 ± 0.4 | 5.2 ± 0.2 | 4.2 ± 0.3 | 6.2 ± 0.2 | 1.5 ± 0.2 | 14.8 ± 1.4 | 6–7 | Large cysts in the gills of *Pseudoplatystoma fasciatum* | Pantanal wetland, Brazil |
| *H. pseudo-platystoma* | 33.2 ± 1.9 | 10.4 ± 0.6 | 3.4 ± 0.4 | – | 3.3 ± 0.4 | 1.0 ± 0.4 | 22.7 ± 1.7 | 6–7 | Gills of hybrid pintado | Fish farms: São Paulo and Mato Grossso do Sul states, Brazil |
| *H. corruscans* | 27.6 | 14.3 | 5.0 | – | 6.8 | 2.0 | 13.7 | 5–6 | Gills of *Pseudoplatystoma corruscans* | Paraná River, Brazil |
| *H. eirasi* | 37.1 ± 1.8 | 12.9 ± 0.8 | 3.4 ± 0.3 | 3.1 ± 0.1 | 5.4 ± 0.5 | 0.7 ± 0.1 | 24.6 ± 2.2 | 12–13 | Gill filaments of *Pseudoplatystoma corruscans* and *Pseudoplatystoma fasciatum* | Pantanal wetland, Brazil |
| *H. maculosus* | 31.2 | 13.7 ± 0.6 | 4.1 ± 0.2 | 3.0 ± 0.3 | 5.6 ± 0.5 | 1.6 ± 0.2 | 17.5 ± 0.5 | 6–7 | Gill filaments of *Pseudoplatystoma corruscans* | Pantanal wetland, Brazil |
| *H. maculosus* | 33.0 | 13.3 ± 0.7 | 4.4 ± 0.4 | 3.5 ± 0.4 | 5.2 ± 0.6 | 1.6 ± 0.2 | 19.7 ± 0.6 | 6–7 | Gill filaments of *Pseudoplatystoma reticulatum* | Pantanal wetland, Brazil |

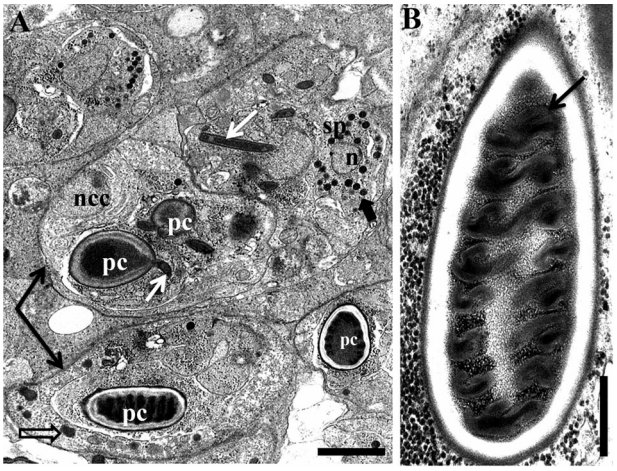


Fig. 2. Ultrastructure of skin of *Phractocephalus hemioliopterus* infected by *Myxobolus figueirae* sp. nov. (A) Sporogenesis process showing sporoblasts (black arrows) with polar capsule (pc), nucleus of the capsulogenic cell (ncc) and polar tubule still not internalized (white arrow), esporoplasm (sp) and nuclei of the sporoplasm (n), sporoplasmosomes (large black arrow) and forming valve material (empty arrow). Scale bar = 2 µm. (B) Polar capsule with polar tubule (black arrow). Scale bar = 500 nm

showed that the thin connective tissue layer (6.7 µm) surrounding the plasmodium was composed of fibroblasts and collagen fibers (Fig. 4A,B). The plasmodial membrane presented numerous pinocytotic canals originating outside of the plasmodia to the ectoplasm zone (Fig. 4C). Numerous mitochondria and electron-translucent vacuoles, either empty or with amorphous electron-dense material were observed in the ectoplasm, while generative cells and several developmental stages of sporogenesis were seen in the inner layers (Fig. 4A). Immature and mature spores were more prevalent in the center of the plasmodium (Fig. 4A).

**Genetics:** Sequencing of the SSU-rDNA from *M. figueirae* sp. nov. spores obtained from a single plasmodium resulted in a 1909 bp sequence with no close matches to any myxosporean species sequences available in GenBank. Pairwise analysis considering only the *Myxobolus* species forming the clade with *M. figueirae* sp. nov. showed that *Myxobolus axelrodi* Camus et al., 2017, possessed 14% difference and was thus the species most genetically similar to the new species. Conversely, *Myxobolus prochilodus* Eiras et al., 2014 possessed 19.5% difference and was the species with the largest genetic divergence (Table 2).

**Prevalence:** 3 of the 7 specimens (42.8%) of *Phractocephalus hemioliopterus* examined were infected.

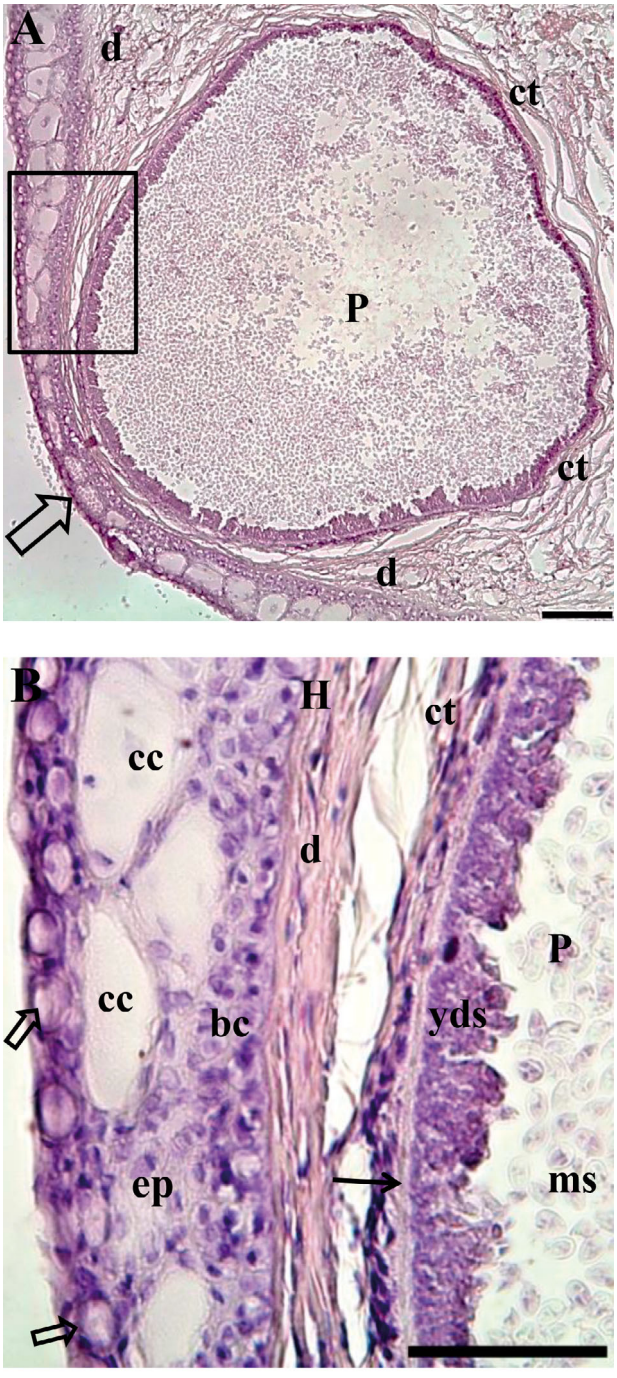


Fig. 3. Histology of skin of *Phractocephalus hemioliopterus* infected by *Myxobolus figueirae* sp. nov. (A) Plasmodium (P) in the dermis (d) surrounded by a connective tissue layer (ct) leading to the stretching of the epidermis layer (empty arrow). Scale bar = 100 µm. (B) Higher magnification of box in (A) showing epidermis (ep) of the host (H) with mucus cells (empty arrows), club cells (cc) and basal cells (bc), and dermis (d) and connective tissue (ct) surrounding the plasmodial wall (thin arrow). Inside the plasmodium (P) there is a peripheral layer of young developmental stages (yds) and inner mature spores (ms). Scale bar = 50 µm

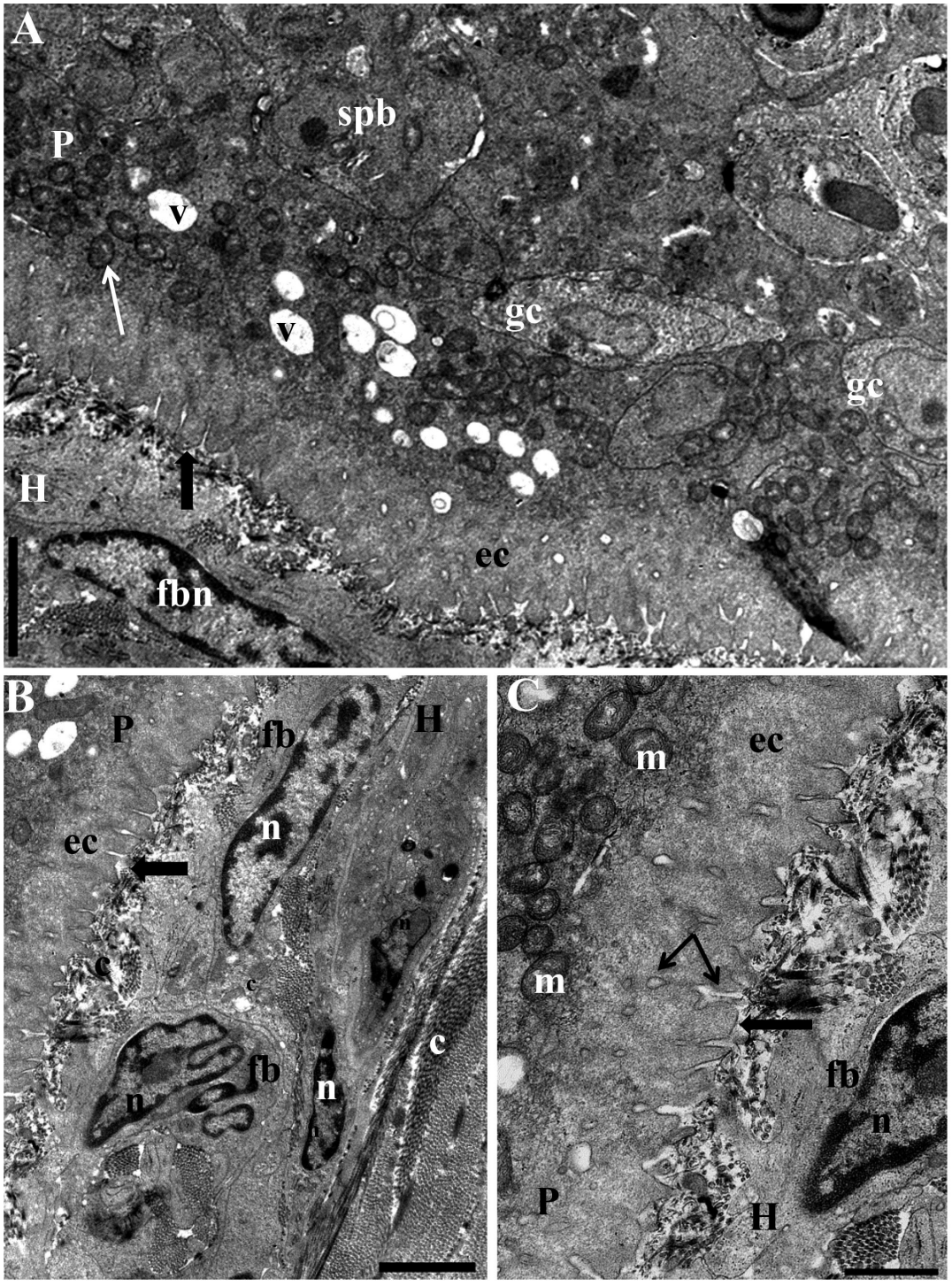


Fig. 4. Ultrastructure of *Phractocephalus hemioliopterus* skin infected by *Myxobolus figueirare* sp. nov. (A) Host–parasite interface showing the wall (large black arrow) of the plasmodium (P). In the ectoplasm (ec), near the plasmodial wall can be observed vesicles (v), mitochondria (white arrow), germinative cells (gc) and sporoblasts (spb). Host (H), fibroblast nuclei (fbn). Scale bar = 10 µm. (B) Magnification of parasite–host interface, showing the collagen layer (c) and fibroblasts (fb) with their nuclei (n) isolating the plasmodium (P) from the host tissue. Plasmodial wall (large black arrow); ectoplasm (ec). Scale bar = 2 µm. (C) Magnification of parasite–host interface, showing plasmodial wall formed by a single membrane (thick black arrow), which features delicate projections and recesses. In ectoplasm (ec) were observed many mitochondria (m) and around the wall were observed pinocytosis channels (thin arrows) connecting to the outside of ectoplasm plasmodium. Host (H); fibroblast (fb) and nuclei of the fibroblast (n). Scale bar = 1 µm

**Site of infection:** Skin.

**Type host:** *P. hemioliopterus* Bloch & Schneider, 1801

**Specimens deposited:** Glass slides with fixed, stained spores (syntype) were deposited in the Museum of Zoology 'Adão José Cardoso', of University of Campinas (UNICAMP), São Paulo, Brazil (accession no. ZUEC MYX 70). The 18S rDNA sequence was deposited in GenBank under accession number MG181226.

**Locality:** Tapajós River, municipality of Santarém, Pará State, Brazil.

**Etymology:** The specific name is in honor of Antônio Sousa Figueira, an expert on the region of the Tapajós River who has critically helped in our fieldwork.

**Remarks:** Unequal polar capsule is a common feature observed in spores of species of the *Myxobolus* genus (Eiras et al. 2005, 2014). Likewise, *M. figueirae* sp. nov. shares this characteristic with several others *Myxobolus* species, of which *Myxobolus sangei* Fonema et al. 2007, was most closely related with respect to the length and width of the spore (Eiras et al. 2005, 2014). Nevertheless, *M. sangei* differs from the new species based on the longer and wider polar capsules (6.2 × 2.2 and 4.8 × 1.7 µm) and by the distinct host family (African Characidae) (Fonema et al. 2007). All other *Myxobolus* species bearing unequal polar capsules differed from *M. figueirae* sp. nov. based on at least one of the characteristics, such as shape and size of spores and polar capsules, number of polar tubule coils or host and tissue affinity (Table 1). BLAST analysis showed that *M. axelrodi* was a species bearing unequal polar capsules and was the closest relative to *M. figueirae* sp. nov. with only 86% similarity, as well as possessing larger spores (20.5 × 6 × 6 µm) and pyriform body shape. Thus, based on morphological and SSU-rDNA data, the species studied here is considered a novel taxon.

### *Henneguya santarenensis* sp. nov.

**Morphology:** Plasmodia, white and elongated, measuring up to 450 µm long. Mature spores, ellipsoidal in the frontal view, 26.3–36.1 (31.9 ± 3) µm in total length, 9.6 to 11.9 (10.8 ± 0.5) µm in body length, 3.7 to 4.9 (4.3 ± 0.3) µm in width and 16.6 to 25.6 (21 ± 3.1) µm in caudal process. Spores biconvex in lateral view, 3.4 to 3.7 (3.6 ± 0.2) µm in thickness and valves symmetrical. Polar capsules, elongated and equal in size, 3.8 to 5.5 (4.6 ± 0.4) µm in length and 1 to 1.7 (1.4 ± 0.2) µm in width (Fig. 1B,D, Table 1). The polar capsules occupy half of the body of the spore, and the anterior ends are adjacent (Fig. 1B,D). The polar tubules have 15 coils and are perpendicular to the longitudinal axis of the polar capsule (Fig. 5).

Histological analysis showed the young plasmodia clearly intralamellar. Mature plasmodia might give the impression of an interlamellar development but actually, their development occurred between the gill lamellar epithelium and the capillary, leading to the stretching of the epithelium, displacement and deformation and lamellar fusion (Fig. 6A). A fibroblast layer was observed surrounding the plasmodium (Fig. 6B). Ultrastructure analysis showed a layer of fibroblasts surrounding the plasmodial wall (Fig. 7A,B). Numerous pinocytosis channels ending in vesicles were observed linking the outside to the ectoplasm zone of the plasmodia (Fig. 7C). Inside, generative cells, pansporoblasts in different developmental stages were present as well as developing and mature spores (Figs. 5 & 7A).

**Genetics:** Molecular analysis of the SSU-rDNA isolated from *H. santarenensis* sp. nov. spores obtained from a single plasmodium resulted in a sequence with 1967 nucleotides, and according to BLAST, did not match any myxosporean species sequences available in GenBank. Pairwise analysis considering only the *Henneguya* species clustering in the clade with *H. santarenensis* sp. nov. showed that *Henneguya cuniculator* Naldoni et al., 2014, with a difference of 7.8% was the species with the smallest genetic divergence to the species described here, while *Henneguya eirasi* Naldoni et al., 2011, with a difference of 13%, showed the largest genetic divergence (Table 3).

**Prevalence:** 7 of the 7 specimens (100%) of *P. hemioliopterus* were infected.

**Site of infection:** Gill lamella.

**Type host:** *P. hemioliopterus* Bloch & Schneider, 1801.

**Specimens deposited:** Glass slides with fixed, stained spores (syntype) were deposited in the Museum of Zoology 'Adão José Cardoso', of University of Campinas (UNICAMP), São Paulo, Brazil (accession no. ZUEC MYX 69). The 18S rDNA sequence was deposited in GenBank under accession number MG181225.

**Locality:** Tapajós River, municipality of Santarém, Pará State, Brazil.

**Etymology:** The species name is based on the type locality, municipality of Santarém.

**Remarks:** Morphological comparison showed some similarity among *H. santarenensis* sp. nov. and other South American *Henneguya*: *H. maculosus* Carriero et al., 2013 has similar spore morphology, total length, width and thickness of the spores, length and

Table 2. Similarity matrix for small subunit ribosomal DNA (SSU-rDNA) of *Myxobolus figueirae* sp. nov. and myxosporean species parasites of characiforms and siluriforms clustered in the same clade as *M. figueirae* sp. nov. Upper right shows nucleotide differences in relation to the number of bases compared; lower left shows % pairwise distance identity

| Species (GenBank no.) | Table ID | 1 | 2 | 3 | 4 | 5 | 6 | 7 | 8 | 9 |
|---|---|---|---|---|---|---|---|---|---|---|
| *M. figueirae* sp. nov. MG181226 | 1 | – | 206/1324 | 301/1868 | 217/1314 | 280/1774 | 290/1912 | 296/1816 | 261/1534 | 331/1786 |
| *M. umidus* KF296350 | 2 | 15.9 | – | 147/1310 | 136/1303 | 204/1312 | 185/1316 | 438/1325 | 199/1019 | 270/1360 |
| *M. hilarii* KM403404 | 3 | 16.5 | 11.3 | – | 115/1300 | 262/1766 | 262/1861 | 301/1810 | 276/1526 | 328/1775 |
| *M. piraputangae* KF296351 | 4 | 16.8 | 10.5 | 8.9 | – | 199/1305 | 183/1306 | 234/1323 | 207/1005 | 251/1354 |
| *M. aureus* KF296348 | 5 | 16.2 | 15.7 | 15.0 | 15.4 | – | 133/1761 | 297/1766 | 284/1468 | 314/1742 |
| *M. batalhensis* MF361090 | 6 | 15.5 | 14.2 | 14.2 | 14.1 | 7.6 | – | 308/1814 | 276/1532 | 321/1781 |
| *M. porofilus* KR528449 | 7 | 16.7 | 18.0 | 17.0 | 18.1 | 17.1 | 17.3 | – | 225/1451 | 261/1787 |
| *M. curimatae* KP120979 | 8 | 18.0 | 20.5 | 19.0 | 21.3 | 20.2 | 18.9 | 16.1 | – | 84/1373 |
| *M. prochilodus* KR528450 | 9 | 19.5 | 20.9 | 19.3 | 19.6 | 18.9 | 18.8 | 15.3 | 6.3 | – |
| *M. omari* EU643624 | 10 | 15.1 | 13.5 | 16.2 | 15.3 | 14.6 | 14.6 | 17.0 | 18.5 | 19.3 |
| *M. physophilus* KY421105 | 11 | 14.4 | 16.0 | 15.2 | 16.7 | 15.4 | 15.3 | 16.7 | 18.1 | 19.6 |
| *M. voremkhai* KY229919 | 12 | 16.5 | 16.0 | 16.4 | 16.6 | 14.9 | 15.9 | 17.0 | 18.4 | 18.0 |
| *M.* cf. *colossomatis* KF597017 | 13 | 15.4 | 18.7 | 16.7 | 17.6 | 13.6 | 14.3 | 14.3 | 17.8 | 19.2 |
| *M. macroplasmodialis* KF296357 | 14 | 15.2 | 17.8 | 17.0 | 16.9 | 16.1 | 15.3 | 17.3 | 18.8 | 20.1 |
| *M. axelrodi* KU936091 | 15 | 14.0 | 14.7 | 14.3 | 17.7 | 14.6 | 13.6 | 16.2 | 18.3 | 16.2 |

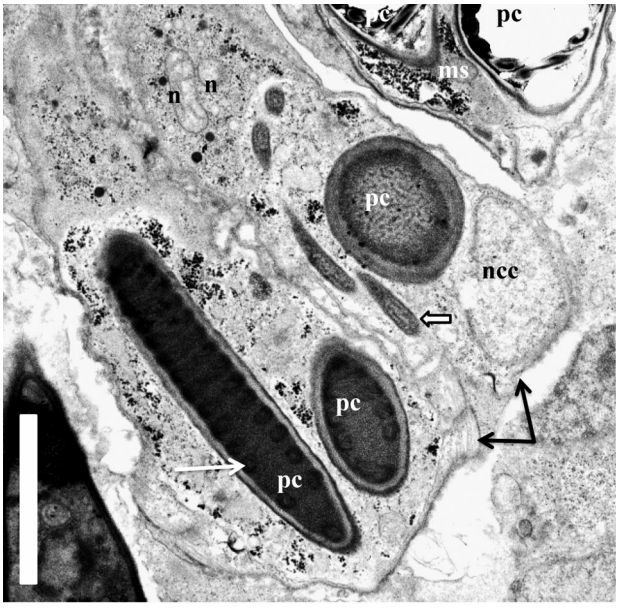


Fig. 5. Ultrastructure of *Phractocephalus hemioliopterus* gill infected by *Henneguya santarenensis* sp. nov. Diasporic formation (thin arrows) showing the polar capsule (pc) with polar tubule internalized (white arrow) and not yet internalized (empty arrow), nuclei of the capsulogenic cells (ncc) and nuclei of the sporoplasm (n). Mature spore (ms). Scale bar = 2 µm

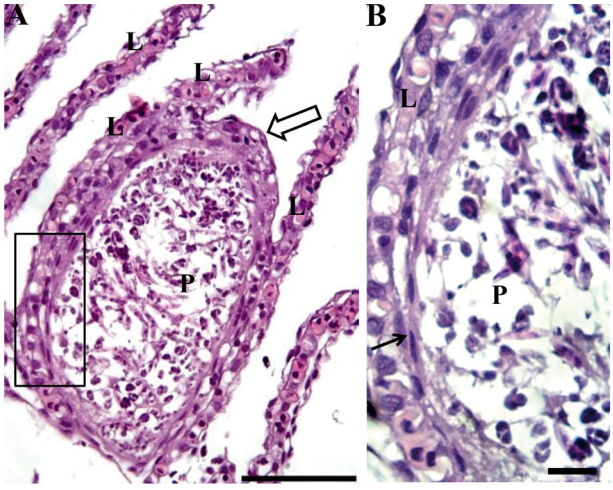


Fig. 6. Gill lamella (L) of *Phractocephalus hemioliopterus* infected by *Henneguya santarenensis* sp. nov. (A) Plasmodium (P) with intraepithelial development causing stretching of the epithelium (empty arrow) and light lamellar fusion. Scale bar = 100 µm. (B) Higher magnification of box in (A) showing the fibroblast layer (thin arrow) separating the plasmodium (P) from the lamella (L). Scale bar = 10 µm

width of the polar capsule and site of infection. However, specific characteristic differences such as smaller body, longer tail, larger number of polar tubule coils and as well as different host species distinguish them. *H. multiplasmodialis* Adriano et al., 2012 resembles *H. santarenensis* sp. nov. in spore morphology, total length, width and thickness of the spores, width of the polar capsule and site of infection, but it differs with respect to body spore size and polar capsules (smaller in *H. santarenensis* sp. nov.), tail length (longer in the new species), different number of coils of the polar tubules, different host species and different morphology of the plasmodia. *H. cuniculator* Naldoni et al., 2014 resembles *H. santarenensis* sp. nov. in the spore width, polar capsule diameter and site of infection, but differs in the tail length in body spore length size (longer in the new

| 10 | 11 | 12 | 13 | 14 | 15 |
|---|---|---|---|---|---|
| 142/962 | 274/1958 | 314/1949 | 204/1364 | 226/1528 | 262/1907 |
| 115/867 | 207/1353 | 207/1341 | 204/1128 | 197/1121 | 190/1319 |
| 152/959 | 278/1905 | 299/1897 | 221/1363 | 254/1526 | 261/1864 |
| 130/864 | 215/1347 | 213/1336 | 191/1127 | 185/1121 | 229/1304 |
| 138/957 | 268/1801 | 260/1791 | 180/1366 | 251/1524 | 254/1768 |
| 138/957 | 289/1947 | 300/1936 | 190/1359 | 231/1522 | 255/1911 |
| 161/959 | 300/1837 | 303/1829 | 190/1364 | 260/1542 | 288/1935 |
| 171/964 | 265/1538 | 269/1546 | 209/1250 | 255/1495 | 266/1532 |
| 180/958 | 337/1786 | 306/1796 | 253/1404 | 295/1548 | 288/1815 |
| – | 104/962 | 118/967 | 131/961 | 154/957 | 128/959 |
| 10.9 | – | 164/2001 | 189/1391 | 252/1554 | 266/1961 |
| 12.4 | 8.3 | – | 211/1381 | 260/1549 | 293/1953 |
| 14.1 | 14.2 | 15.9 | – | 190/1361 | 185/1363 |
| 16.3 | 16.7 | 17.3 | 14.4 | – | 216/1524 |
| 13.5 | 14.0 | 15.4 | 14.0 | 14.5 | – |

species), polar capsule (shorter in the new species), different number of polar tubule coils and different host species. Thus, based on morphological and molecular sequence differences, the above species is proposed as a new taxon.

### Phylogenetic analysis

Our phylogenetic analysis based on the closest myxozoan sequences to each one of the species studied (based on GenBank data), showed *H. santarenensis* sp. nov. clustering in a well-supported subclade composed by *Henneguya* species that infect gills of the South American pimelodid host (Fig. 8). Conversely, *M. figueirae* sp. nov. appears weakly supported in a subclade containing parasites of varying organs of South American bryconid hosts (Fig. 8).

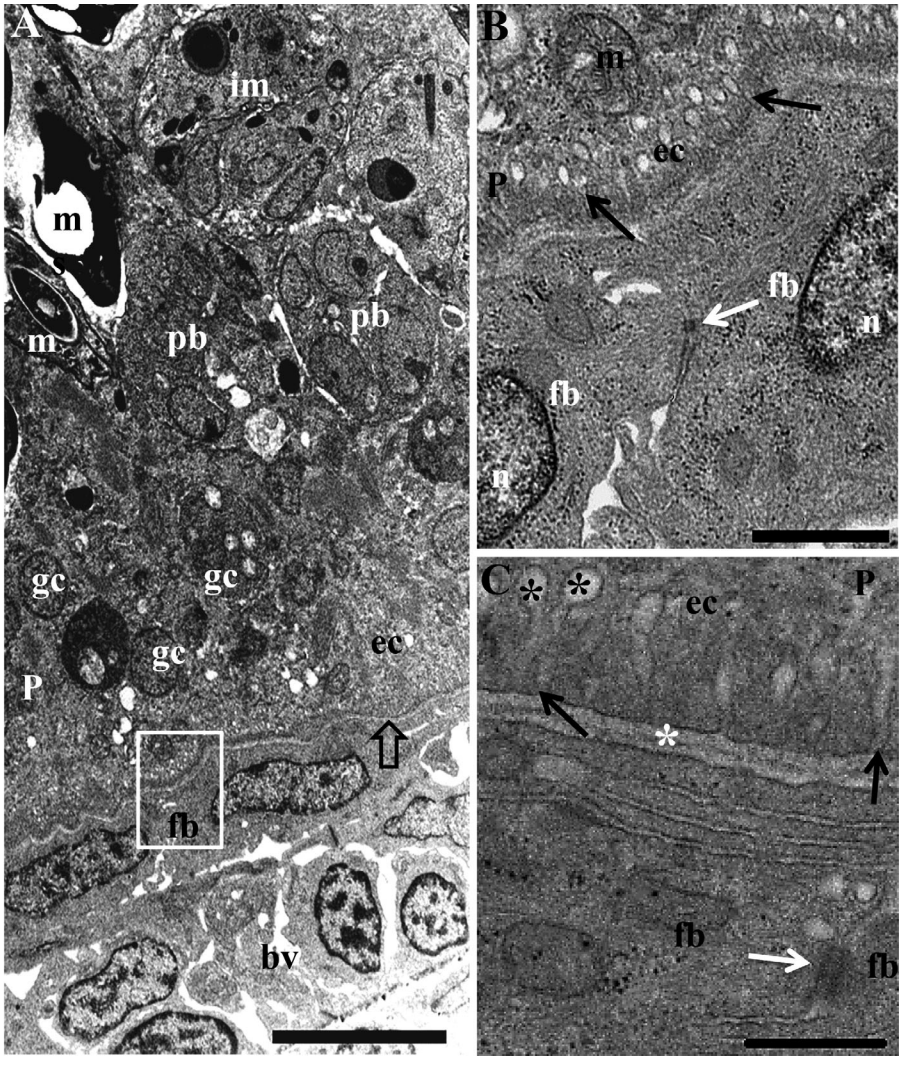


Fig. 7. Ultrastructure of *Phractocephalus hemioliopterus* gill infected by *Henneguya santarenensis* sp. nov. (A) Host–parasite interface showing a layer of fibroblasts (fb) between the blood vessel (bv) and the plasmodial wall (large arrow). Inside the plasmodium (P) there is an ectoplasm zone (ec) followed by a layer with generative cells (gc), pansporoblasts in different developmental stages (pb) and immature (im) and mature (m) spores. Scale bar = 5 µm. (B) Magnification of box in (A), showing the layer of the fibroblasts (fb) with their nuclei (n) and desmosomal junction (white arrow). In the plasmodial (P) side is seen the ectoplasm (ec) with numerous pinocytosis channels (black arrows) and a mitochondrion (m). Scale bar = 500 nm. (C) Higher magnification of the host–parasite interface showing a desmosomal junction (white arrow) of the fibroblasts (fb), granular material occupying the space between the plasmodial wall and the fibroblast layer (white asterisk), details of the plasmodial wall with pinocytosis channels (black arrows) ending in a vesicle (black asterisk). Scale bar = 500 nm

Table 3. Similarity matrix for small subunit ribosomal-rDNA (SSU-rDNA) of *Henneguya santarenensis* sp. nov. and myxosporean species parasites of pimelodids clustered in the same subclade as *H. santarenensis* sp. nov. Upper right shows nucleotide differences in relation to the number of bases compared; lower left shows % pairwise distances identity

| Species (GenBank no.) | Table ID | 1 | 2 | 3 | 4 | 5 | 6 | 7 |
|---|---|---|---|---|---|---|---|---|
| *H. santarenensis* sp. nov. MG181225 | 1 | – | 94/1221 | 144/1338 | 209/1923 | 155/1215 | 211/1947 | 241/1951 |
| *H. cuniculator* KF732840 | 2 | 7.8 | – | 22/1214 | 53/1215 | 50/1214 | 136/1222 | 162/1220 |
| *H. multiplasmodialis* KF296354 | 3 | 11.0 | 1.8 | – | 109/1559 | 187/1210 | 241/1592 | 200/1340 |
| *H. corruscans* KF296356 | 4 | 11.0 | 4.2 | 7.0 | – | 193/1206 | 259/1938 | 248/1929 |
| *H. eirasi* KF296355 | 5 | 13.0 | 11.8 | 15.9 | 16.4 | – | 111/1209 | 144/1212 |
| *H. maculosus* KF296344 | 6 | 11.0 | 11.3 | 15.5 | 13.7 | 9.2 | – | 183/1942 |
| *H. pseudoplatystoma* KP981638.1 | 7 | 12.4 | 13.4 | 15.2 | 13.1 | 12.0 | 9.5 | – |

## DISCUSSION

Only around 100 myxosporean species have been described from South American freshwater environments, the majority belonging to the genera *Myxobolus* or *Henneguya* (Adriano & Oliveira 2017). This relatively low number is in contrast to the high number of known fish species in these habitats and indicates there are likely many more associated parasite species to be identified and described. Despite the economic importance of *Phractocephalus hemioliopterus* to the Amazon fishing industry and in the aquarium sector, this is the first report of a myxosporean infecting this species.

The histological and ultrastructural analysis of both *Myxobolus figueirae* sp. nov. and *Henneguya santarenensis* sp. nov. showed a common feature of myxosporean infections, i.e. the absence of inflammatory infiltrate, but the presence of connective tissue layer surrounding the plasmodia (Sitjà-Bobadilla 2008). In addition, significant tissue alterations were observed in gills infected by *H. santarenensis* sp. nov., including compression, deformation and fusion of adjacent lamellae. Conversely, in skin infected by *M. figueirae* sp. nov., only a light stretching of the epidermis was observed. Similar tissue changes have been reported in other myxosporean gill and epithelial infections (e.g. Molnár 1998, Özer et al. 2016, Ali Dar et al. 2017), including infections of other species in pimelodid hosts (Naldoni et al. 2009, 2011, 2014, Adriano et al. 2012).

Ultrastructural analysis revealed that the plasmodial membrane of both *M. figueirae* sp. nov. and *H. santarenensis* sp. nov. presented pinocytotic canals originating outside of the plasmodia toward the ectoplasm zone. In *H. santarenensis* sp. nov., these pinocytotic canals end in a dilated vesicle; these characteristics have also been reported in other myxosporean species (Azevedo & Matos 2002, 2003, Adriano et al. 2005b). In *H. santarenensis* sp. nov., a delicate layer of finely granular material prevented contact between the layer of fibroblasts and plasmodial membrane, a characteristic also observed in gill myxosporeans (Müller et al. 2013, Naldoni et al. 2014, 2015). Sporogenesis appeared to follow a common pattern observed in many other myxosporeans species, where generative cells and young developmental stages occur in the periphery of the plasmodium and the immature and mature spores are found in the center (Hallett & Diamant 2001, Casal et al. 2002, Adriano et al. 2005a,b, 2006).

In South America, studies concerning SSU-rDNA sequencing of myxosporean parasites of pimelodids are restricted to 8 species, with only *Thelohanellus marginatus* originating from the Amazon. The phylogenetic analysis of partial SSU-rDNA sequences performed in our study showed *Myxobolus*/*Henneguya*/*Unicauda* species and *T. marginatus* grouping in a clade that further divided into 2 distinct lineages in accordance with Capodifoglio et al. (2016). The genus *Myxobolus* is distinguished from *Unicauda* and *Henneguya* by the absence of 1 or 2 caudal processes, and from *Thelohanellus* by the presence of 2 polar capsules rather than 1. However, these morphological differences were not well supported by molecular data (Fiala et al. 2015). Our study further confirms the findings of Fiala et al. (2015), with an intermingling of *Myxobolus*/*Henneguya*/*Unicauda*/*Thelohanellus* species in different subclades. In this context, despite *M. figueirae* sp. nov. and *H. santarenensis* sp. nov. infecting the same host in the same environment, they clustered in distinct lineages, indicating distinct evolutionary pathways. *H. santarenensis* sp. nov. clustered in a well-supported sub-clade of species parasites of South American pimelodids, which appears as a sister lineage to parasite species of North American ictalurids, forming a large clade of parasites of siluriform hosts. Mean-

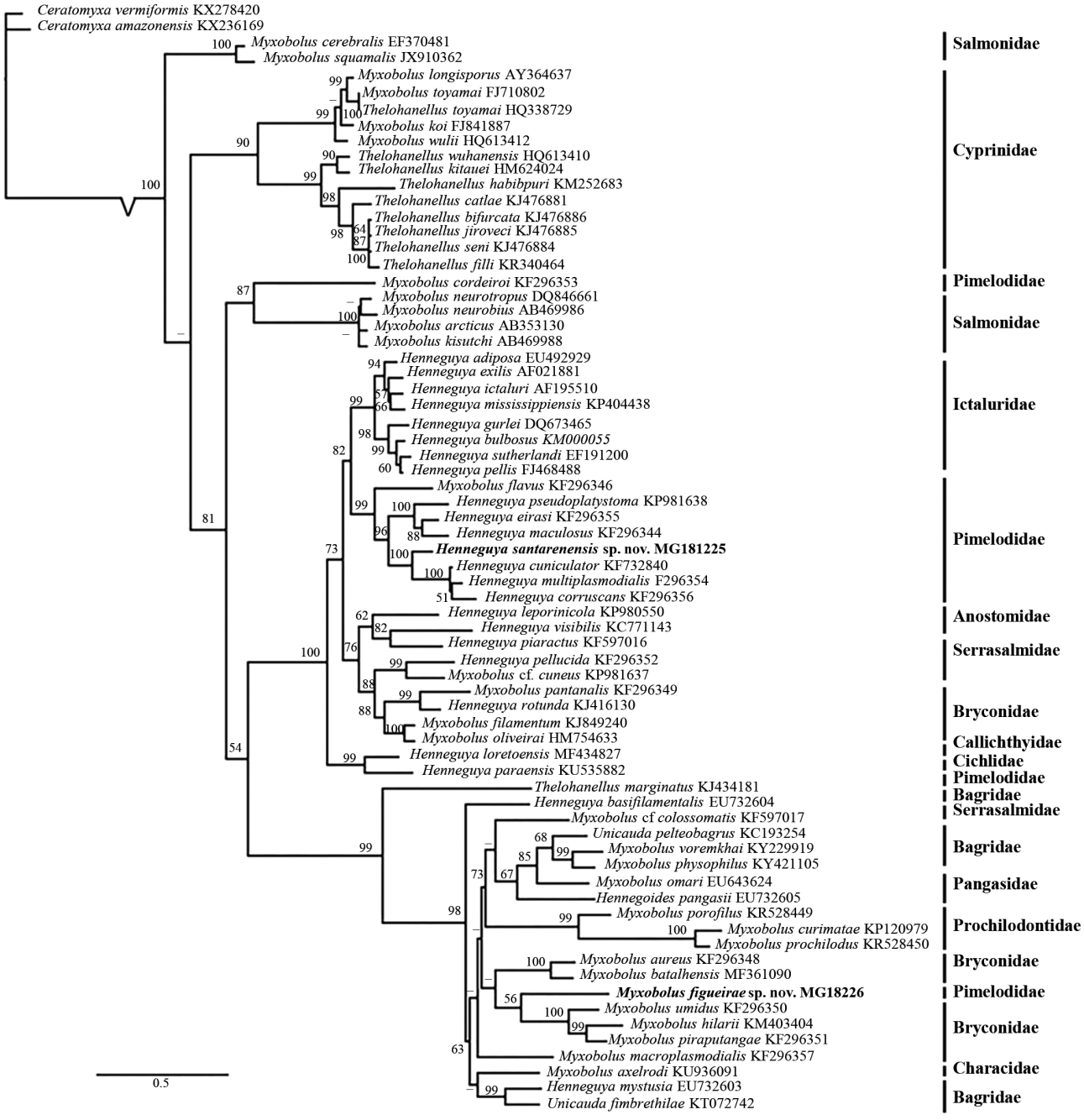


Fig. 8. Maximum likelihood tree showing the relationship between *Myxobolus figueirae* sp. nov. and *Henneguya santarenensis* sp. nov. described in this study and the closest myxozoan sequences deposited in GenBank based on partial small subunit ribosomal DNA (SSU-rDNA). Numbers above nodes indicate bootstrap confidence levels (>50%) from maximum likelihood

while, *M. figueirae* sp. nov. clustered in a weakly supported subclade comprised of parasites species of bryconids hosts. This position of *M. figueirae* sp. nov. together with that observed of *T. marginatus* and *Myxobolus cordeiroi* Adriano et al. 2009, suggests that myxobolid parasites of pimelodids are not monophyletic. Further indicating that the host–parasite systems composed by *M. figueirae* sp. nov., *M. cordeiroi* and *T. marginatus* may have been a result of switches in host.

This study describes 2 new myxosporean species from the Amazon biome, increasing our knowledge of biodiversity in that region, as well as offering new insights on the evolution of host–parasite relationships of myxosporean parasites of *P. hemioliopterus*, an economically important pimelodid fish species across South America.

*Acknowledgements*. The authors thank Ashlie Hartigan for suggestions on the paper and Gareth Porteous for the English revision. This study was supported by the São Paulo Research Foundation - FAPESP (Proc. No. 2013/21374-6 - Adriano EA). J.N. was supported by a post-doctoral scholarship from FAPESP (Proc. No. 2014/22700-7). E.A.A. received a research productivity grant from the Brazilian Fostering Agency CNPq (Proc. No.305630/2013-0).

## LITERATURE CITED

Adriano EA, Oliveira OMP (2017) Myxosporea in catálogo taxonômico da fauna do Brasil. http://fauna.jbrj.gov.br/fauna/faunadobrasil/152799 (accessed 23 May 2017)

Adriano EA, Arana S, Cordeiro NS (2005a) Histology, ultrastructure and prevalence of *Henneguya piaractus* (Myxosporea) infecting the gills of *Piaractus mesopotamicus* (Characidae) cultivated in Brazil. Dis Aquat Org 64: 229–235

Adriano EA, Arana S, Cordeiro NS (2005b) An ultrastructural and histopathological study of *Henneguya pellucida* n. sp. (Myxosporea: Myxobolidae) infecting *Piaractus mesopotamicus* (Characidae) cultivated in Brazil. Parasite 12:221–227

Adriano EA, Arana S, Cordeiro NS (2006) *Myxobolus cuneus* n. sp. (Myxosporea) infecting the connective tissue of *Piaractus mesopotamicus* (Pisces: Characidae) in Brazil: histopathology and ultrastructure. Parasite 13:137–142

Adriano EA, Carriero MM, Maia AAM, Silva MRM, Naldoni J, Ceccarelli OS, Arana S (2012) Phylogenetic and host–parasite relationship analysis of *Henneguya multiplasmodialis* n. sp. infecting *Pseudoplatystoma* spp. in Brazilian Pantanal wetland. Vet Parasitol 185:110–120

Ali Dar S, Kaur H, Chishti MZ (2017) *Myxobolus chushi* n. sp. (Myxozoa:Myxosporea) parasitizing *Schizothorax niger* (Heckel), a native cyprinid fish from Wullar Lake in Kashmir Himalayas. Parasitol Int 66:272–278

Altschul SF, Madden TL, Schaffer AA, Zhang J, Zhang Z, Miller W, Lipman DJ (1997) Gapped BLAST and PSI-BLAST: a new generation of protein database search programs. Nucleic Acids Res 25:3389–3402

Azevedo C, Matos E (2002) Fine structure of the myxosporean, *Henneguya curimata* n. sp., parasite of the Amazonian fish, *Curimata inormata* (Teleostei, Curimatidae). J Eukaryot Microbiol 49:197–200

Azevedo C, Matos E (2003) Fine structure of *Henneguya pilosa* sp. n. (Myxozoa: Myxosporea), parasite of *Serrasalmus altuvei* (Characidae), in Brazil. Folia Parasitol 50: 37–42

Barassa B, Adriano EA, Cordeiro NS, Arana S, Ceccarelli PS (2012) Morphology and host–parasite interaction of *Henneguya azevedoi* n. sp., parasite of gills of *Leporinus obtusidens* from Mogi-Guaçu River, Brazil. Parasitol Res 110:887–894

Barta JR, Martin DS, Liberato PA, Dashkevicz M and others (1997) Phylogenetic relationships among eight *Eimeria* species infecting domestic fowl inferred using complete small subunit ribosomal DNA sequences. J Parasitol 83: 262–271

Capodifoglio KRH, Adriano EA, Milanin T, Silva MRM, Maia AAM (2016) Morphological, ultrastructural and phylogenetic analyses of *Myxobolus hilarii* n. sp. (Myxozoa, Myxosporea), a renal parasite of farmed *Brycon hilarii* in Brazil. Parasitol Int 65:184–190

Carriero MM, Adriano EA, Silva MRM, Ceccarelli PA, Maia AAM (2013) Molecular phylogeny of the *Myxobolus* and *Henneguya* genera with several new South American species. PLOS ONE 8:e73713

Casal G, Matos E, Azevedo C (2002) Ultrastructural data on the spore of *Myxobolus maculatus* n. sp. (phylum Myxozoa), parasite from the Amazonian fish *Metynnis maculatus* (Teleostei). Dis Aquat Org 51:107–112

Eiras JC, Adriano EA (2012) A checklist of new species of *Henneguya* Thélohan, 1892 (Myxozoa: Myxosporea, Myxobolidae) described between 2002 and 2012. Syst Parasitol 83:95–104

Eiras JC, Molnár K, Lu YS (2005) Synopsis of the species of *Myxobolus* Bütschli, 1882 (Myxozoa: Myxosporea: Myxobolidae). Syst Parasitol 61:1–46

Eiras JC, Zhang J, Molnár K (2014) Synopsis of the species of *Myxobolus* Bütschli, 1882 (Myxozoa: Myxosporea: Myxobolidae) described between 2005 and 2013. Syst Parasitol 88:11–36

Feist SW, Longshaw M (2006) Phylum Myxozoa. In: Woo PTK (ed) Fish diseases and disorders. Protozoan and metazoan infections, Vol. 1, 2nd edn. CAB International, Wallingford, p 230–296

Fiala I, Bartošová-Sojková P, Okamura B, Hartikainen H (2015) Adaptive radiation and evolution within the Myxozoa. In: Okamura B, Gruhl A, Bartholomew JL (eds) Myxozoan evolution, ecology and development. Springer, Cham, p 69–84

Fonema A, Lekeufack Folefack GB, Tang C II (2007) New species of *Myxobolus* (Myxosporea: Myxobolidae) parasites of fresh water fishes in Cameroon (Central Africa). J Biol Sci 7:1171–1178

Froese R, Pauly D (eds) (2013) FishBase. www.fishbase.org (accessed Nov 2017)

Goulding M (1996) Pescarias Amazônicas, proteção de habitats e fazendas nas Várzeas: uma visão ecológica e econômica. Relatório técnico para o projeto 'Manejo dos recursos naturais da Várzea'. IBAMA, Brasília

Guindon S, Dufayard JF, Lefort V, Anisimova M, Hordijk W, Gascuel O (2010) New algorithms and methods to estimate maximum-likelihood phylogenies: assessing the performance of PhyML 3.0. Syst Biol 59:307–321

Hall TA (1999) BioEdit: a user-friendly biological sequence alignment editor and analysis program for Windows 95/98/NT. Nucleic Acids Symp Ser 41:95–98

Hallett SL, Diamant A (2001) Ultrastructure and small-subunit ribosomal DNA sequence of *Henneguya lesteri* n. sp (Myxosporea), a parasite of sand whiting *Sillago analis* (Sillaginidae) from the coast of Queensland, Australia. Dis Aquat Org 46:197–212

Lundberg JG, Littmann MW (2003) Family Pimelodidae (Long-whiskered catfish). In: Reis ER, Kullander SO, Ferraris CJ Jr (eds) Check list of the freshwater fishes of South and Central America. Edipucrs, Porto Alegre, p 432–446

Lundberg JG, Sullivan JP, Hardman M (2011) Phylogenetics of the South American catfish family Pimelodidae (Teleostei, Siluriformes) using nuclear and mitochondrial gene sequences. Proc Acad Nat Sci Philadelphia 161: 153–189

Matos E, Tajdari J, Azevedo C (2005) Ultrastructural studies of *Henneguya rhamdia* n. sp. (Myxozoa) a parasite from the Amazon teleost fish, *Rhamdia quelen* (Pimelodidae). J Eukaryot Microbiol 52:532–537

Molnár K (1998) Taxonomic problems, seasonality and histopathology of *Henneguya creplini* (Myxosporea) infection of the pikeperch *Stizostedion lucioperca* in Lake Balaton. Folia Parasitol 45:261–269

Molnár K, Eszterbauer E, Székely C, Dán A, Harrach B (2002) Morphological and molecular biological studies on intramuscular *Myxobolus* spp. of cyprinid fish. J Fish Dis 25:643–652

MPA (Ministério da Pesca e Aqüicultura) (2012) Boletim estatístico da pesca e aquicultura. Ministério da Pesca e Aquicultura, Brasília

Müller MI, Adriano EA, Ceccarelli PS, Silva MRM, Maia AAM, Ueta MT (2013) Prevalence, intensity, and phylogenetic analysis of *Henneguya piaractus* and *Myxobolus* cf. *colossomatis* from farmed *Piaractus mesopotamicus* in Brazil. Dis Aquat Org 107:129–139

Naldoni J, Arana S, Maia AAM, Ceccarelli PS and others (2009) *Henneguya pseudoplatystoma* n. sp. causing reduction in epithelial area of gills in the farmed pintado, a South American catfish: histopathology and ultrastructure. Vet Parasitol 166:52–59

Naldoni J, Arana S, Maia AAM, Silva MRM and others (2011) Host–parasite–environment relationship, morphology and molecular analyses of *Henneguya eirasi* n. sp. parasite of two wild *Pseudoplatystoma* spp. in Pantanal Wetland, Brazil. Vet Parasitol 177:247–255

Naldoni J, Maia AAM, Silva MRM, Adriano EA (2014) *Henneguya cuniculator* sp. nov., a parasite of spotted sorubim *Pseudoplatystoma corruscans* in the São Francisco Basin, Brazil. Dis Aquat Org 107:211–221

Naldoni J, Zatti SA, Capodifoglio KRH, Milanin T, Maia AAM, Silva MRM, Adriano EA (2015) Host-parasite and phylogenetic relationships of *Myxobolus filamentum* sp. n. (Myxozoa: Myxosporea), a parasite of *Brycon orthotaenia* (Characiformes: Bryconidae) in Brazil. Folia Parasitol 62:014

Okamura B, Gruhl A, Bartholomew JL (2015) An introduction to myxozoan evolution, ecology and development. In: Okamura B, Gruhl A, Bartholomew JL (eds) Myxozoan evolution, ecology and development. Springer, Cham, p 1–22

Özer A, Özkan H, Gürkanlı CT, Yurakhno V, Çiftçi Y (2016) Morphology, histology and phylogeny of *Henneguya sinova* sp. nov. (Mybobolidae: Myxozoa) infecting gills of *Parablennius tentacularis* in the Black Sea, Turkey. Dis Aquat Org 118:207–215

Rambaut A (2008) FigTree v1.1.1: tree figure drawing tool. http://tree.bio.ed.ac.uk/software/figtree/ (accessed 16 Mar 2014)

Rocha S, Casal G, Velasco M, Alves A, Matos E, Al-Quraishye S, Azevedo C (2014) Morphology and phylogeny of *Thelohanellus marginatus* n. sp. (Myxozoa: Myxosporea), a parasite infecting the gills of the fish *Hypophthalmus marginatus* (Teleostei: Pimelodidae) in the Amazon River. J Eukaryot Microbiol 61: 586–593

Santos GM (1986/1987) Composição do Pescado e situação da pesca no Estado de Rondônia. Acta Amaz 17:43–84

Sitjà-Bobadilla A (2008) Fish immune response to myxozoan parasites. Parasite 15:420–425

Tamura K, Stecher G, Peterson D, Filipski A, Kumar S (2013) MEGA 6: molecular evolutionary genetics analysis version 6.0. Mol Biol Evol 30:2725–2729

Val AL, Honczaryk A (1995) Criando peixes na Amazônia, 19 edn. INPA, Manaus

Zhang ZQ (2011) Animal biodiversity: an introduction to higher-level classification and taxonomic richness. Zootaxa 3148:7–12

*Editorial responsibility: Dieter Steinhagen, Hannover, Germany*

*Submitted: May 8, 2017; Accepted: January 12, 2018*
*Proofs received from author(s): March 10, 2018*